61

Report on a study of the EC radiation scheme

J. Slingo

Research Department

July 1982

1. INTRODUCTION

Before starting on the development of a cloud parameterization scheme it seemed important that the method and performance of the radiation scheme should be understood as fully as possible. To this end a detailed study of the scheme has been made and its performance assessed using the single column model with an initial profile derived from GATE data. The behaviour of the scheme near sharp inversions was also considered using a profile from ATEX (Atlantic Trade Experiment). The following aspects of the scheme were studied in some detail:-

(i) Clear-sky fluxes and heating rates.

(ii) The effect of the vertical smoothing of humidity on the treatment of inversions.

(iii) Fluxes and heating rates associated with clouds at various levels. The bulk radiative properties of the clouds are calculated and compared with other estimates.

(iv) The effect of changing the specification of cloud liquid water on the heating rates, fluxes and the bulk radiative properties of the clouds.

2. CLEAR SKY FLUXES AND HEATING RATES

The characteristics of the radiation scheme in clear-sky conditions were studied using the GATE mean profile shown in Fig. 1. The ascent is moist, particularly near the surface. For the purposes of this study the scheme was altered to print out the various components of the solar and infrared fluxes. Heating rates were also divided into short wave and long wave.

Under clear-sky conditions the scheme's treatment of the absorption and scattering of solar radiation seems satisfactory. The main discrepancy with other estimates is in the solar heating rates in the lower troposphere (Fig. 2). Here the scheme gives considerably more heating by at least 0.5 K day^{-1} and is questionable for the following reason. In the troposphere the main absorber of solar radiation is water vapour. As the solar radiation penetrates lower into the troposphere the energy in the water vapour bands is progressively removed, until they are almost completely absorbed. Thus in the lower troposphere, although the humidity mixing ratio increases, the rate of absorption should decrease. Such a decrease is seen in the other estimates but not in the EC scheme. The reason for this discrepancy lies in the form of the transmission function used. In Fig. 3 the water absorptivity curve as a function of absorber amount is compared with those used by Slingo and Schrecker (1982) and Lacis and Hansen (1974). The EC scheme agrees well with the other curves at low absorber amounts but deviates

significantly for large path lengths. In the lower tropical troposphere absorber amounts are typically near 10 g cm^{-2} so that the absorptivity curve used in the EC scheme will overestimate the absorption in this region. This would seem to explain the large heating rates obtained with the EC scheme.

The solar fluxes computed by the EC scheme show a reasonable reflectivity (10%) but, as expected from the heating rates, the absorbed flux is too high (32% of the incoming flux). Vonder Haar and Hanson (1969) quote observed values of 17-19% for a clear atmosphere in 0-10N and the scheme of Slingo and Schrecker (1982) gives 18% for the GATE profile used in this study. Consequently the EC scheme has too little solar radiation reaching the surface (277 Wm^{-2} compared with 323 Wm^{-2} from Slingo and Schrecker) and this could have important consequences for the land surface heat balance.

The upward and downward infrared fluxes computed by the EC scheme in clear-sky conditions have been compared with various observed and modelled values from GATE given in Table 1 taken from Rowntree (1981). Details of the observations and the models are given in Table 2. The upward fluxes agree well with the modelled and observed values in the lower and middle troposphere. Above 400 mb however, the EC scheme gives upward fluxes that are systematically lower than the majority of the other values. Similar values were obtained from the ATEX profile (Fig. 6) which is considerably drier, so it does not seem to be related to the humidity profile. The cause of the discrepancy seems to be in the calculation of the ozone transmissivity in much the same way as was found for the short wave water vapour transmission. The downward fluxes are in reasonable agreement with the various models and observations bearing in mind their large variability.

The infrared cooling rates from the scheme are shown in Fig. 4 along with those from the scheme of Roach and Slingo (1979), using the same data, and an observed profile from the Line Islands Experiment (Cox, 1969). The main difference is the lack of cooling maximum near the surface in the EC scheme. This is due to the neglect of the continuum in the computation of the gaseous transmission. The continuum or dimer has an absorption coefficient (k) which is dependent on the water vapour pressure (e) with the form

$$k = k_1 p + k_2 e \qquad \text{(Bignell, 1970)} \qquad (2.1)$$

where the first term is the pressure broadening term. Typically, $K_1 = 0.004$ g^{-1} cm^{-2} atm^{-1}. Paltridge and Platt (1976) point out that in the atmospheric window the approximate contributions to the radiance of the pressure broadening term, the vapour pressure term and the other gases

are, respectively, 15%, 70% and 15%. The main problem in incorporating the dimer effect in the scheme is the computation of the mean water vapour pressure encountered by the radiation. The results of a first attempt at including the continuum effect in the EC scheme are shown in Fig. 5. The water vapour transmissivity (τ) between 9.07 and 12.27 μm has been replaced by the term:-

$$\tau = \exp\left[-(k_1\phi_1(T)p + k_2\phi_2(T)e)u\right] \qquad (2.2)$$

where $\phi_1 = (\frac{263}{T})^{-1.5}$ and $\phi_2 = (\frac{263}{T})^{6.5}$, u is the absorber amount (Roach and Slingo, 1979). For simplicity the local value for e was used. Although there is increased cooling and a higher outgoing flux - both improvements - the increased cooling penetrates too high into the troposphere. This may be due to the use of a local e rather than a pathlength weighted mean vapour pressure. However, the dimer effect is sufficiently important that some way of including it in the scheme should be found.

3. THE EFFECT OF VERTICAL SMOOTHING OF HUMIDITY ON THE TREATMENT OF INVERSIONS

The humidity mixing ratios used in the radiation scheme are determined from the saturated mixing ratio at the k-levels multiplied by the relative humidity averaged over three adjacent levels. In most circumstances the effect of this is small but the physical implications near atmospheric inversions warrant some consideration. The radiative effects of the smoothing were studied using a profile from ATEX (Fig. 6) which contains a fairly sharp lower tropospheric inversion with relatively dry air aloft. The effect of the vertical smoothing on the infrared and solar clear-sky heating rates is shown on Fig. 7. In neither case does the scheme respond very strongly to the inversion particularly in the infrared. The effect of the smoothing is to shift the level of increased cooling from below to the inversion to above the inversion thus leading to a reduction rather than an enhancement in the strength of the inversion. It is generally considered, however, that, except where the overlying air is relatively moist, the effect of radiation is to strengthen an inversion (Staley, 1965). The small response of the infrared part of the scheme to a large humidity and temperature change is somewhat surprising. Could it be related to the approximations used in the derivation of the long wave flux equation used in the scheme ? The equation involved an assumption relating the isothermal case to the temperature dependent case via the term ε^*:-

$$F = \pi B + (F^o - F^o/\varepsilon^*)\,\tau + (F^o/\varepsilon^* - \pi B)\frac{\tau - 1}{\ln\tau} \qquad (3.1)$$

where F^o is the flux without gaseous absorption, πB is the local black body flux

and ε^* is the emissivity corresponding to the fluxes computed in the isothermal case. This equation also includes the assumption that the black body fluxes vary linearly with optical depth. It is not clear that either this assumption or the assumption that ε^* can be applied to the temperature dependent case are valid in the vicinity of sharp temperature and humidity gradients.

In addition, a 'cooling to space' approximation has been used to derive equation (3.1). This means that the terms representing exchange with the surface and internal exchange with other layers in the atmosphere have been largely neglected. The last term on the right hand side of equation (3.1) represents an approximation for the internal exchange term based on the assumption that the black body flux is a linear function of optical depth. However, in the vicinity of inversions the internal exchange term is important (Rodgers and Walshaw, 1966) and the approximations used in the scheme may prove inadequate. There may be other circumstances where the approximation falls short, for example, in the stratosphere where exchange, in the atmospheric window, between the surface and the ozone layers may be significant. There may also be problems with this approximation near clouds though this aspect needs further study.

4. EFFECT OF CLOUDS ON FLUXES AND RADIATIVE HEATING RATES

The radiative effects of high, medium and low layer clouds have been studied by placing varying amounts of cloud in the 50 mb layers centred on 250, 550 and 850 mb. Only one cloud was considered at a time. The net radiative cooling in the cloud layer as a function of cloud amount is shown in Fig. 8. All the clouds show a rapid increase in radiative cooling for small cloud amounts. This rather intense reaction to small cloud amounts could lead to problems in the model through the response of the convection and the cloud parameterization. The slight decrease in radiative cooling with increasing cloud cover seen for medium cloud seems physically unrealistic. In Fig. 9(a) the dependence of the outgoing flux at the top of the atmosphere on cloud cover again shows unphysical behaviour for all clouds. With the GATE profile, all the clouds are colder than the surface and so should decrease the outgoing flux because they block off the warmer surface. As can be seen, the error is greatest for high cloud. The downward infrared flux at the surface (Fig. 9(b)) is reasonable, the response of the clouds being dependent on the temperature of the cloud relative to the effective temperature of the clear-sky flux.

The radiative properties of high, medium and low layer clouds have been computed by alternately placing a cloud cover of 100% at different levels in the atmosphere. The levels chosen were 850, 550 and 250 mb. The cloud filled a single layer and was always 50 mb deep.

The computed short wave reflectivities and absorptivities, defined according to the amount of energy reaching the cloud top, are shown in Table 3 where they are compared with estimates from various sources. The results show that, for all clouds, the EC scheme gives rather low reflectivities and absorptivities. These results could have some bearing on those reported by Geleyn et al. (1982) where they noted rather low values of albedo in the EC model in the trade wind areas. The reflectivities of these stratocumulus clouds are probably underestimated by the scheme.

In the infrared the behaviour of clouds is more complicated because as well as absorbing and scattering the incident radiation they are also themselves sources of radiation. They emit at the local temperature of the cloud with an emissivity which should be close to unity for most water clouds (Stephens, 1978) but may be a lot less for ice clouds (Liou and Wittman, 1979). The infrared effect of clouds in the EC scheme has been studied by comparing the fluxes at the cloud boundaries with the appropriate black body flux. The results are shown in Table 4. Low cloud is behaving almost as a black body although it is interesting to note that the flux from the cloud top is less than either the black body flux or the flux entering the cloud base, presumably due to the scattering effects of the cloud. Medium cloud also has an emissivity close to unity, particularly for the downward flux. As already noted, high cloud behaves in rather an unexpected fashion. Instead of reducing the upward flux it increases it. This behaviour is not supported by satellite observations over areas of high cloud and may account for the high values of IR emittance noted by Geleyn et al. (1982) in the region of the ITCZ.

5. THE SENSITIVITY OF THE CLOUD RADIATIVE PROPERTIES TO CHANGES IN THE LIQUID WATER CONTENT

At present the cloud liquid water is calculated assuming a supersaturation of 0.2%. This typically gives liquid water contents that are at least an order of magnitude lower than those quoted by Cox and Griffith (1979) and Stephens (1978). In this study the scheme has been altered to compute liquid water contents with supersaturations of 1% and 2%. The values given by Cox and Griffith (1979) have also been used. The effects of these changes on the short wave properties of the clouds are shown in Table 5. For low and medium clouds the increase in liquid water gives a sharp rise in reflectivity but has a minimal effect on the absorptivity. This appears to be for two reasons; firstly that the cloud is low in the atmosphere so that much of the energy in the water vapour bands has already been removed and secondly that as the reflectivity increases, the radiation available for absorption is reduced. The second reason presumably accounts for the decrease in absorptivity seen with all the clouds as the

liquid water content increases. Nevertheless, apart from high cloud, the absorptivities are still considerably lower than those quoted in Table 3. For medium and low cloud Cox and Griffith's values of liquid water content give reflectivities that are too high with the present parameterization of cloud optical properties. The most satisfactory results would be obtained with a value of liquid water content based on slightly less than a supersaturation of 1%. However, it might be instructive to test other parameterizations of optical depth and single scattering albedo such as those given by Stephens (1978) and Slingo and Schrecker (1982). For high cloud the use of a supersaturation of 2% seems reasonable although it should be borne in mind that these are ice crystal clouds and therefore might require a different treatment. At the moment no distinction is made in the scheme between ice and water clouds.

The infrared effects of altering the liquid water content are shown in Table 6. For low and medium clouds the scattering properties of the clouds are more evident with an increase in $F_B\downarrow$ over and above the black body flux and a decrease in $F_T\uparrow$. The most dramatic effect of increasing the liquid water content is on the behaviour of the high cloud. The cloud now shows a decrease in the outgoing flux and with a liquid water content based on a supersaturation of 2% behaves very much like a cirrus cloud with an emissivity of 0.5 - a value currently used in a number of general circulation models.

The effect of increasing the liquid water content to the recommended values on the radiative cooling in the cloud layer is shown in Fig. 10. The increase in cooling for small cloud amounts is now even more dramatic and both medium and high cloud show unphysical decreases in radiative cooling with increasing cloud cover. The effects of scattering were thought to be responsible and so, as a test, the single scattering albedo for high cloud was reduced by three orders of magnitude. The effect on the fluxes and heating rates was dramatic. Instead of a radiative cooling the cloud now experiences a radiative warming (Fig. 11) as observed by Fimpel et al. (1977). The outgoing flux is much improved (Fig. 12a)) although the decrease in the flux to the surface (Fig. 12(b)) is probably unrealistic and needs further study.

6. PROPOSED AMENDMENTS TO THE EC RADIATION SCHEME

(a) Treatment of gaseous transmission including the dimer effect

In both the short wave and long wave parts of the scheme the gaseous transmission (T) is calculated using the equation:

$$T = 1.0/(1.0 + \frac{1}{\alpha}(Au/\sqrt{1.0+Bu^2/u_r}) + Cu_r)^{\alpha} \qquad (6.1)$$

where u and u_r are the unreduced and reduced pathlengths, A, B and C are temperature dependent functions and α is a constant between 0 and 1, the value depending on whether there is strong or weak line absorption. The present version of the scheme has = 1.0 for reasons of computational economy. However, this represents only weak line absorption and so α was decreased to 0.5. This change gave substantial improvements in both the short wave and long wave. The solar flux reaching the surface increased by 24 Wm^{-2} whilst the outgoing flux increased by 30 Wm^{-2} due to the better treatment of the 9.6 μm band of ozone. The increase in computation time was small being 0.037 seconds for a single sweep of an eighteen level profile.

The term Cu_r in 6.1 represents the continuum effects but is clearly independent of water vapour pressure in the present version of the scheme. However, the formulation of the infrared scheme does not allow a pathlength mean vapour pressure to be correctly calculated (see Section 6 (c)). Instead, the coefficients used to determine C have been adjusted to incorporate implicitly a continuum effect for an atmosphere with 75% relative humidity. This adjustment was only made between 9.07 and 12.27 μm where line absorption is weak. This change resulted in a much greater lower tropospheric cooling (by up to 0.8 K day^{-1}).

The net effect of both these amendments on the radiative heating rates is shown in Fig. 13. The revised scheme has greater cooling at all levels but particularly in the lower troposphere. The solar flux to the surface (S↓) and the outgoing long wave flux (F↑) are both improved but the downward long wave flux to the surface (F↓) is now too small.

(b) Treatment of clouds

The results given in Sections 4 and 5 indicate that an increase in the supersaturation used to calculate cloud liquid water would be advisable. Typically a supersaturation of 1% seems satisfactory for low and medium cloud with 2% for high cloud. These changes improve the cloud short wave reflectivities but the absorptivities still remain too low and further study is needed here.

In the infrared an increase in cloud liquid water and a reduction in scattering give much improved results.

(c) Formulation of the infrared part of the scheme

As discussed in Section 3 several approximations have been necessary in order to keep the scheme computationally economic. These approximations are accurate for an isothermal atmosphere but become less so as the temperature and humidity gradients become sharper. Thus the scheme would seem to work least well near atmospheric inversions and possibly near clouds - precisely those areas where radiation is most important.

Another economy has been made in the calculation of pathlengths where the approximation has been made that the only source term is at the top of the atmosphere as in the solar case. This is correct for an isothermal atmosphere. However, in reality very little infrared radiation originates from the upper atmosphere and for the upward flux, for example, a large part originates from at or near the surface. Thus the pathlengths used to derive the transmissions for the infrared fluxes are seriously in error as can be seen in Fig. 14. Here the pathlengths have been plotted on a logarithmic scale for the downward and upward radiation streams. The pathlengths associated with 100% cloud cover, placed alternately at three levels, are also shown. Clearly, the radiation emitted by the clouds and the surface will not experience the correct transmissivities. This may well account for the rather low values of radiative cooling predicted under cloud decks and explains the lack of success in attempts to include a vapour pressure dependent continuum (Section 2). The dimer only becomes effective near the surface where the scheme does not calculate any pathlengths.

All these results suggest a thorough review of the method for calculating infrared fluxes. Clearly, extending the present scheme to cope explicitly with all the emission terms would be expensive. The possibility of developing an 'emissivity' scheme such as that used in the Meteorological Office general circulation models (Slingo, 1982) was considered. However, this method is now rather 'out-of-date' and has the disadvantage of totally excluding scattering effects. The possibility of developing a scheme based on the exponential-sum fitting of transmissions (ESFT) technique has been considered. This method was developed for treating gaseous absorption in the presence of strong scattering (Wiscombe and Evans, 1977) and represents a viable alternative (in both solar and infrared) to the approach currently used in the EC scheme. With the ESFT technique the total transmission is calculated directly from the layer absorber amounts and the optical depths for clouds and aerosols. This therefore removes the necessity of calculating pseudo-optical depths from the fluxes without gaseous absorption and avoids the problems involved in allowing for the various source terms in the atmosphere (Geleyn and Hollingsworth, 1979).

7. SUMMARY

The scheme is an attractive and efficient way of solving the radiative transfer problem. It has the virtue of accommodating cloud at any level with a parameterization of optical properties that allows the user to amend or experiment with them if desired. The results presented in this brief report show some deficiencies in the scheme which may require major changes, particularly in the infrared part. Below are listed the main results from this study with recommendations for possible changes to the scheme.

(a) Solar heating rates in the lower troposphere are too high by as much as 0.5 K day^{-1}. Consequently the solar flux reaching the surface is too low by 45 Wm^{-2}. The water vapour transmissivity curve should be amended.

(b) Infrared cooling rates in the lower troposphere are too low by as much as 1.5 K day^{-1}. Some way of including the water dimer effect should be found.

(c) Upward infrared fluxes in the upper troposphere and lower stratosphere are considerably lower (by about 40 Wm^{-2}) than observed values. This is related to the specification of the ozone transmissivity.

(d) The scheme does not show much response to atmospheric inversions. How well do the approximations used to derive the long wave fluxes behave in these circumstances ?

(e) Cloud shortwave reflectivities are rather low but are improved with an increase in cloud liquid water content.

(f) Cloud short wave absorptivities are consistently too low. The reasons are not clear but should be investigated.

(g) The behaviour of clouds in the infrared is improved with an increase in cloud liquid water particularly for high cloud. The effects of scattering are very evident and some adjustment of the infrared optical properties might be advisable.

The following remark applies generally to items (e), (f) and (g). Apart from adjusting the cloud liquid water content to more realistic values it might also be worthwhile to test out other parameterizations of cloud optical properties such as those of Stephens (1978) and Slingo and Schrecker (1982).

REFERENCES

Bignell, K.J. 1970 The water vapour infrared continuum. Q.J.R.M.S., 96, 390-403.

Cox, S.K. 1969 Observational evidence of anomalous infrared cooling in a clear tropical atmosphere. J. Atm. Sci., 26, 1347-1349.

Cox, S.K. and Griffith, K.T. 1979 Estimates of radiative divergence during Phase III of the GARP Atlantic Tropical Experiment. J. Atm. Sci., 36, 576-601.

Fimpel, H.P., Kuhn, P.M. and Stearns, L.P. 1977 Measurement of infrared irradiances with radiometersondes during GATE from R.V. 'Meteor', Forsch., Berlin, Reihe B, No. 12, 23-30.

Geleyn, J-F. and Hollingsworth, A. 1979 An economical analytical method for the computation of the interaction between scattering and line absorption of radiation. Contr. to Atmos. Physics, 52, 1-16.

Geleyn, J-F., Hense, A. and Preuss, H.J. 1982 A comparison of model generated radiation fields with satellite measurements. To appear in Contrib. Atm. Phys.

Lacis, A.A. and Hansen, J.E. 1974 A parameterization for the absorption of solar radiation in the earth's atmosphere. J. Atm. Sci., 31, 118-133.

Liou, K.N. 1976 On the absorption, reflection and transmission of solar radiation in cloudy atmospheres, J. Atm. Sci., 33, 798-805.

Liou, K.N. and Wittman, G.D. 1979 Parameterization of the radiative properties of clouds. J. Atm. Sci., 36, 1261-1273.

Paltridge, G.W. and Platt, C.M.R. 1976 Radiative processes in meteorology and climatology. Devel. in Atmos. Sci., 5.

Reynolds, D.W. and others 1975 J. Appl. Met., 14, 433-444.

Roach, W.T. and Slingo, A. 1979 A high resolution infrared radiative transfer scheme to study the interaction of radiation with cloud. Q.J.R.M.S., 105, 603-614.

Rodgers, C.D. and Walshaw, C.D. 1966 The computation of infrared cooling rate in planetary atmospheres. Q.J.R.M.S., 92, 67-92.

Rowntree, P.R. 1981 A survey of observed and calculated long wave fluxes for the cloud-free tropical atmosphere. Met. O 20, Tech. Note No.II/174.

Slingo, J.M. 1982 A study of the earth's radiation budget using a general circulation model. Q.J.R.M.S., 108, 379-406.

Slingo, A. and Schrecker, H.M. 1982 On the shortwave radiative properties of stratiform water clouds. Q.J.R.M.S., 108, 407-426.

Staley, D.O. 1965 Radiative cooling in the vicinity of inversions and the tropopause. Q.J.R.M.S., 91, 282-301.

Stephens, G.L. 1978 Radiation profiles in extended water clouds. J. Atm. Sci., 35, 2111-2132.

Vonder Haar, T.H. and Hanson, J. 1969 J. Atm. Sci., 26, 652-655.

Welch, R.M. and Cox, S.K. 1980 Solar radiation and clouds. Met. Monographs, Vol. 17, No. 39.

Wiscombe, W.J. and Evans, J.W. 1977 Exponential-sum fitting of radiative transmission functions. J. Comp. Phys. 24, 416-444.

TABLE 1

COMPARISONS BETWEEN OBSERVATIONAL AND MODEL LONG WAVE RADIATIVE COOLING RATES FOR CLOUDFREE TROPICAL ATMOSPHERE

(a) Upward fluxes (Wm^{-2})

		Surface	1000	970	900	800	600	400	200	100 mb	Above 100 mb
	(i) Observed										
1	USSR GATE			453	439	418	376	320	251	223	
2	FRG GATE			447	439	425	384	337	287	277	
3	USA BOMEX			455	445	423	379	344	294	281	
4	USA IRI		455		441	415	379	340	298	286	
5	FRG IRI		(468)		431	408	369	324	277	259	
6	JAPAN IRI				442	415	381	335	287	274	
7	GATE Aircraft		462	457	440	420	367	285	230		
	(ii) Models										
8	Fimpel (I)			446	432	409	355	306	258	243	247 (10 mb)
9	Fimpel (II)			446	432	409	365	327	288	280	280 (10 mb)
10	Cox/Griffith		453	447	427	407	350	304	250		
11	Ellingson/Gille	463			428	413	368	329	296	286	
12	Gille/Kuhn		457		430	404	366	324	290	281	278 (40 mb)
13	MO 11-layer	453	450	444	431	412	374	335	302	295	290 (0 mb)
14	MO 5-layer	453	450	444	429	410	370	331	302	297	293 (0 mb)
15	Roach/Slingo	455	455	447	431	408	364	322	288	281	282 (5 mb)
16	ECMWF	460	458	446	431	414	370	322	260	244	240 (0 mb)

TABLE 1

(b) Downward fluxes (Wm^{-2})

			Surface	1000	970	900	800	600	400	200	100 mb	Estimated net surface flux
	(i)	Observed										
1		USSR GATE			404	383	348	279	188	98	70	37
2		FRG GATE			356	340	312	231	152	64	18	79
3		USA BOMEX			418	388	328	243	144	57	36	25
4		USA IRI		427		364	308	236	140	53	31	25
5		FRG IRI		(396)		357	327	245	145	63	36	(72)
6		JAPAN IRI				344	291	217	115	28	12	65
7		GATE aircraft		415	399	365	323	224	146	65		44
	(ii)	Models										
8		Fimpel (I)			396	364	335	248	130	29	11	38
9		Fimpel (II)			356	314	278	202	118	29	9	78
10		Cox/Griffith		437	424	386	327	201	125	37		13
11		Ellingson/Gille	417			353	303	211	117	26	11	46
12		Gille/Kuhn		408		345	291	210	112	25	11	46
13		MO 11-layer	380	370	350	308	253	174	100	24	15	73
14		MO 5-layer	380	372	352	308	254	173	97	28	11	73
15		Roach/Slingo	386	386	368	330	280	197	116	31	16	69
16		ECMWF	385	378	362	332	296	212	123	30	12	75

Notes: See Table 3

TABLE 2

Notes to Table 1

	Abbreviated name	Reference	Atmosphere	Number of Cases	Further information
1	USSR GATE	Feigelson (1980)	GATE	?	'Tropical cloudless' set
2	FRG GATE	Fimpel et al (1977)	GATE (2012Z, 13/8/74)	1	
2A	"	" "	GATE	9	
3	USA BOMEX	Ellingson and Gille (1978)	Discoverer (3/6/69)	1	
4	USA IRI	Gille and Kuhn (1973)	Caribbean, East Pacific (May 1970)	4	
5	FRG IRI	"	"	4	Data in parentheses are for 2 cases
6	Japan IRI	"	"	4	
7	GATE Aircraft	Cox and Griffith (1979)	GATE (25/8/74)	1	
8	Fimpel (I)	Fimpel et al (1977)	GATE (2012Z, 13/8/74)	1	Model I
9	Fimpel (II)	"	"	1	Model II
10	Cox/Griffith	Cox and Griffith (1979)	GATE (25/8/74)	1	
11	Ellingson/Gille	Ellingson and Gille (1978)	Discoverer (3/6/69) Barbados (8/6/69)	2	
12	Gille/Kuhn (1973)	Gille and Kuhn (1973)	Caribbean, East Pacific (May 1970)	4	
13	MO 11-layer	Unpublished	GATE mean	1	Walker (1977)'s model
14	MO 5-layer model	"	"	1	Slingo (1980)'s model (No ozone)
15	Roach/Slingo	"	"	1	Roach and Slingo (1980)'s model (Surface pressure 1000 mb)
16	ECMWF	"	"	1	Geleyn and Hollingsworth (1979)

Table 3 **Comparison of shortwave radiative properties for layer clouds**

Low cloud

	EC scheme	Welch and Cox[x] 1980	Stephens 1978[*]	Liou and Wittman[+] 1979	Liou 1976	M.O. Model (Slingo 1982)
Reflectivity (%)	56	63	65 - 70	40 - 73	45 - 67	70
Absorptivity (%)	3	8	9 - 11	9 - 17	6 - 9	10

x For 500m thick cloud but with solar zenith angle of 0^{o}
* Using Sc 1 case from Fig. 3.
\+ For a range of liquid water contents (0.1 to 0.9 gm^{-3}).

Medium cloud

	EC scheme	Welch and Cox[x] 1980	Stephens 1978[*]	Liou 1976	M.O. Model (Slingo 1982)
Reflectivity	31	61	60 - 78	56	60
Absorptivity	4	11	9 - 11	15	10

x For 500m thick cloud but with solar zenith angle at 0^{o}.
* Using As case from Fig. 3.

High cloud

	EC scheme	Welch and Cox[+] 1980	Reynolds et al. 1975	M.O. Model (Slingo 1982)
Reflectivity	2	1 - 75	47 - 59	20
Absorptivity	3	7 - 58	13 - 15	5

\+ Dependent on particle size and shape

Table 4 Infra-red fluxes at cloud boundaries

	Upward fluxes (Wm^{-2})				Downward fluxes (Wm^{-2})		
	$F_T^{\uparrow}$	B_T	$F_B^{\uparrow}$		$F_B^{\downarrow}$	B_B	$F_T^{\downarrow}$
Low cloud	389	393	427		405	406	305
Medium cloud	311	293	364		298	309	180
High cloud	296	143	283		88	173	38

F_T - Flux at cloud top

F_B - " " cloud base

B_T - Black body flux at cloud top

B_B - " " " " " base

Table 5 Effect of changing liquid water content on cloud shortwave properties

Low cloud

Liquid water content	Reflectivity	Absorptivity	Transmissivity
0.002 q_s	56	3	41
0.01 q_s	85	3	12
0.02 q_s	91	3	6
1.0×10^{-3} *	96	3	1

Medium cloud

0.002 q_s	31	5	64
0.01 q_s	71	4	25
0.02 q_s	82	3	15
0.265×10^{-3} *	91	3	6

High cloud

0.002 q_s	2	3	95
0.01 q_s	9	6	85
0.02 q_s	18	8	74
0.035×10^{-3} *	58	7	35

* Values taken from Cox and Griffith (1979)

Table 6 Effect of changing cloud liquid water on infra-red fluxes at cloud boundaries

Low cloud

Liquid water content	$F_T^{\uparrow}$	B_T	$F_B^{\uparrow}$		$F_B^{\downarrow}$	B_B	$F_T^{\downarrow}$
0.002 q_s	389	393	427		405	406	305
0.01 q_s	387	393	427		409	406	305
0.02 q_s	386	393	427		409	406	305
1.0×10^{-3}	386	393	427		409	406	305

Medium cloud

0.002 q_s	311	293	364		298	309	180
0.01 q_s	286	293	364		316	309	180
0.02 q_s	285	293	364		317	309	180
0.265×10^{-3}	285	293	365		317	309	180

High cloud

0.002 q_s	296	143	283		88	173	38
0.01 q_s	268	143	283		123	173	38
0.02 q_s	227	143	283		147	173	38
0.035×10^{-3}	148	143	283		186	173	38

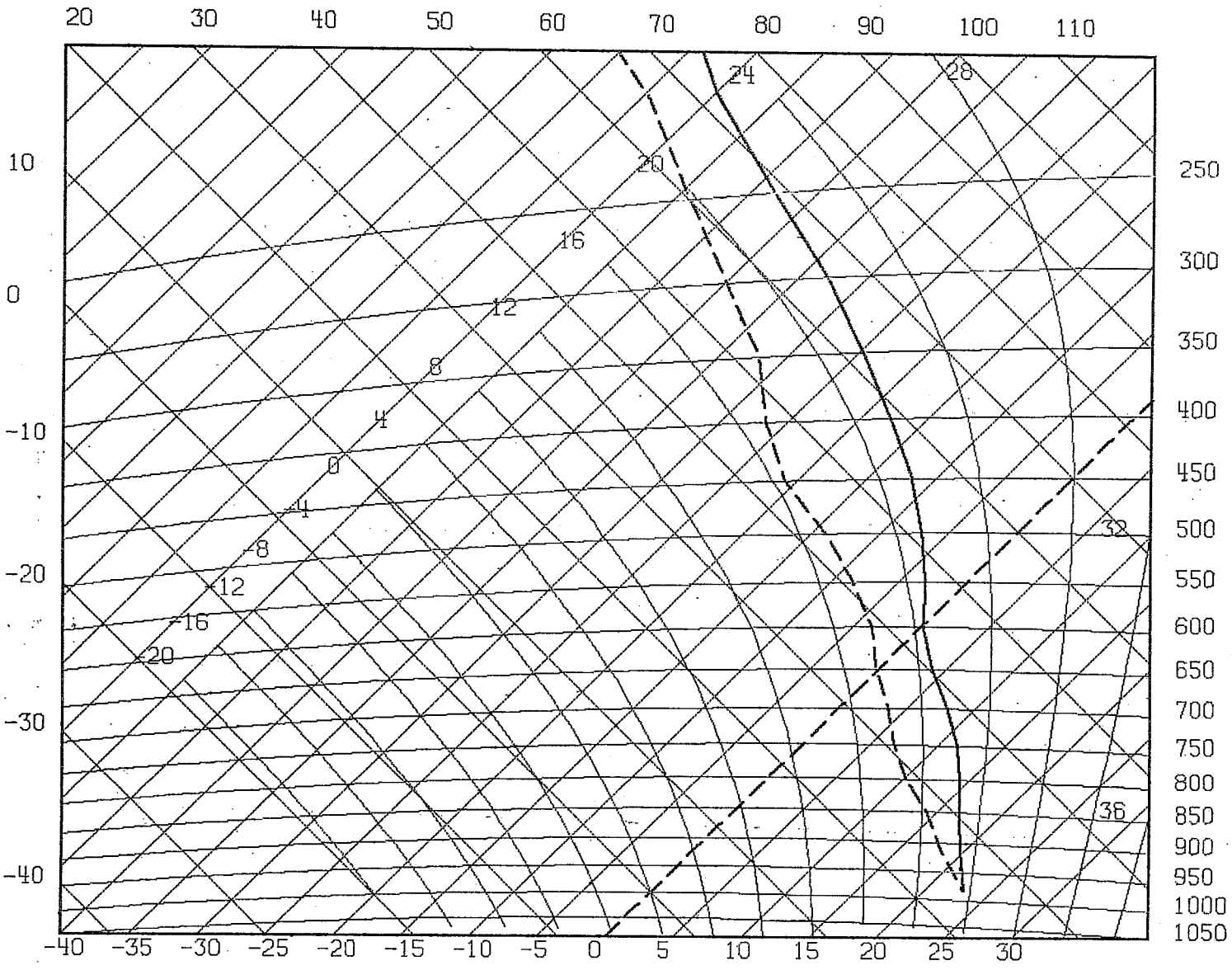

Fig. 1 GATE profile.

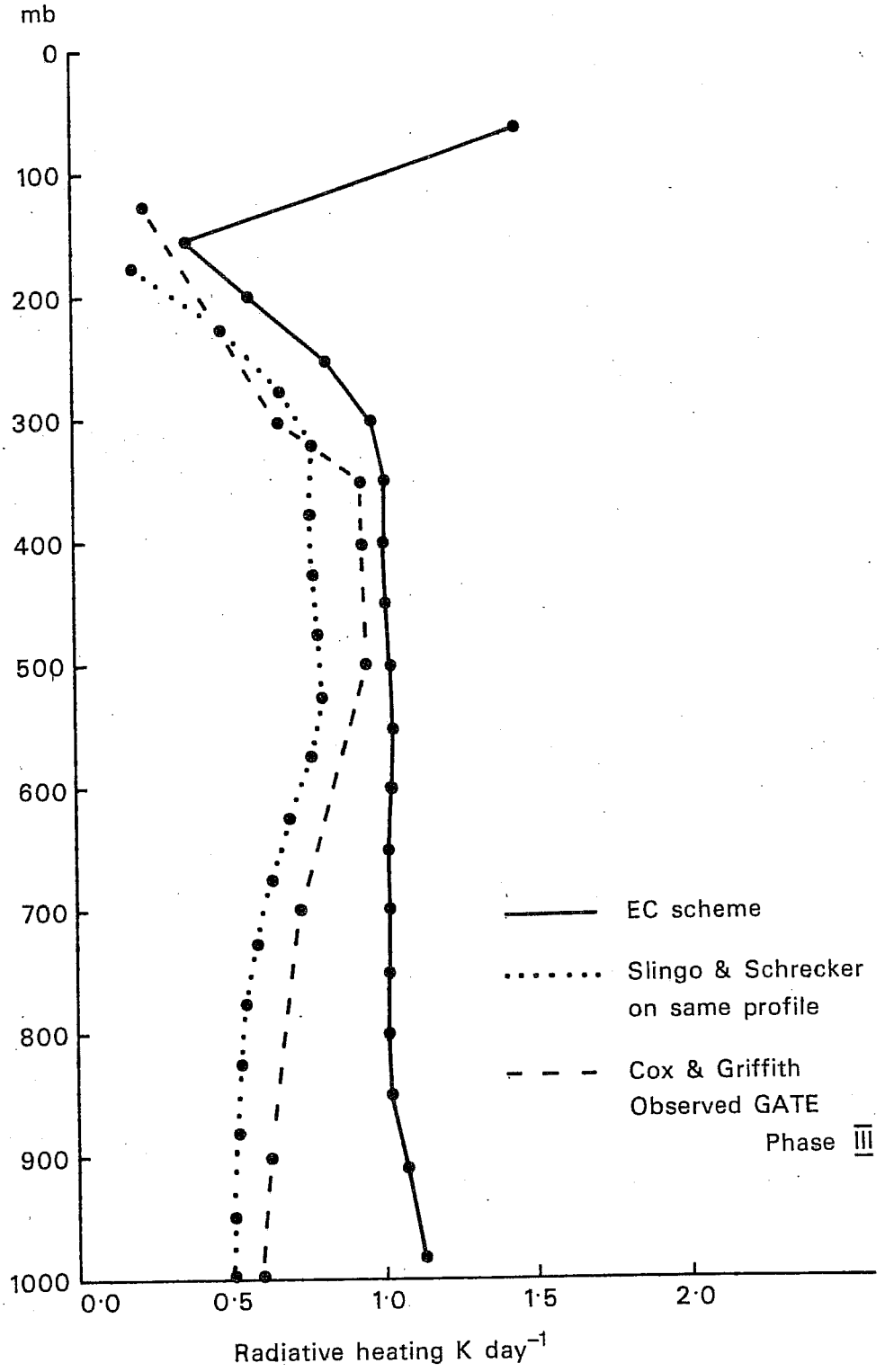

Fig. 2 Comparison of solar heating rates from EC scheme with other estimates.

(0·217) ×

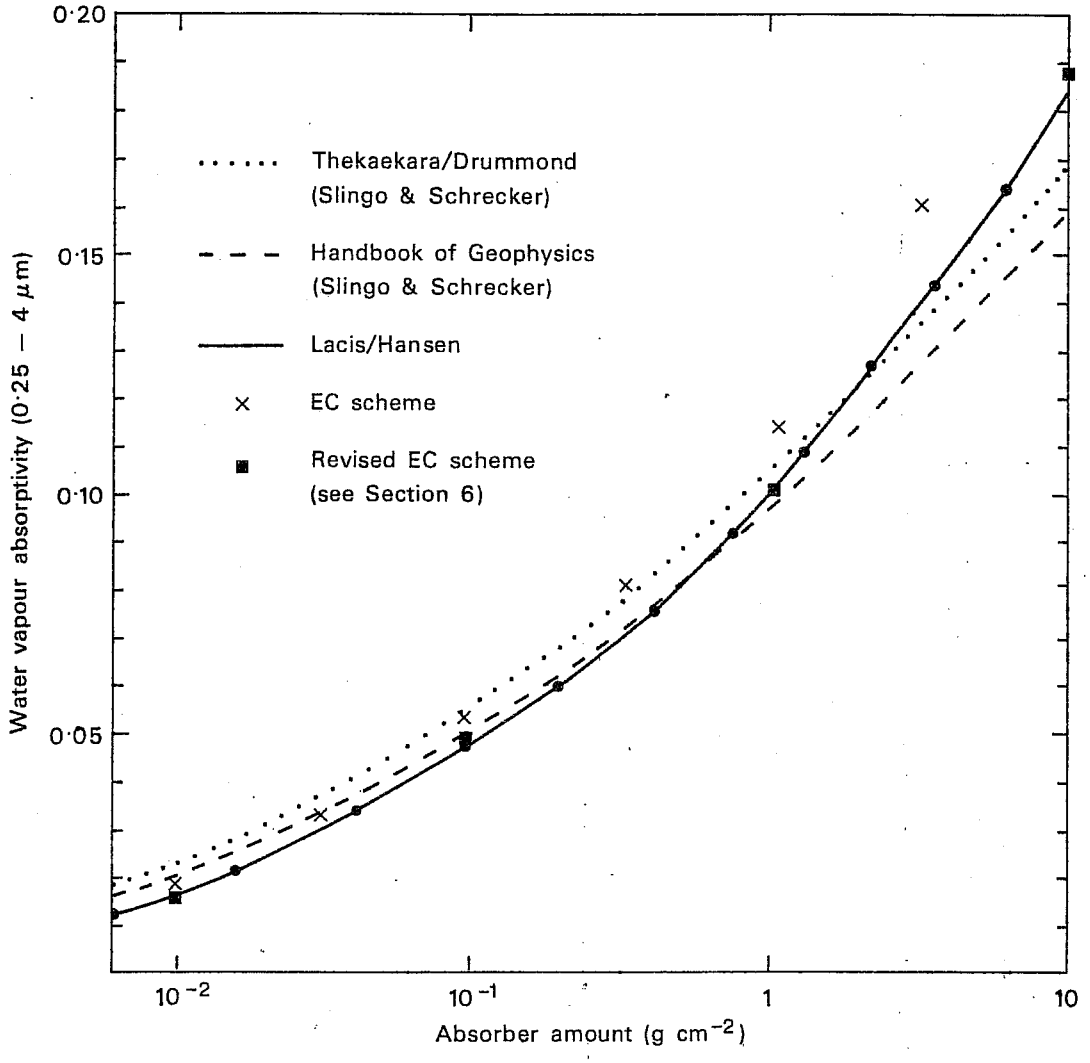

Fig. 3 Comparison of water vapour absorptivity in EC scheme with other estimates.

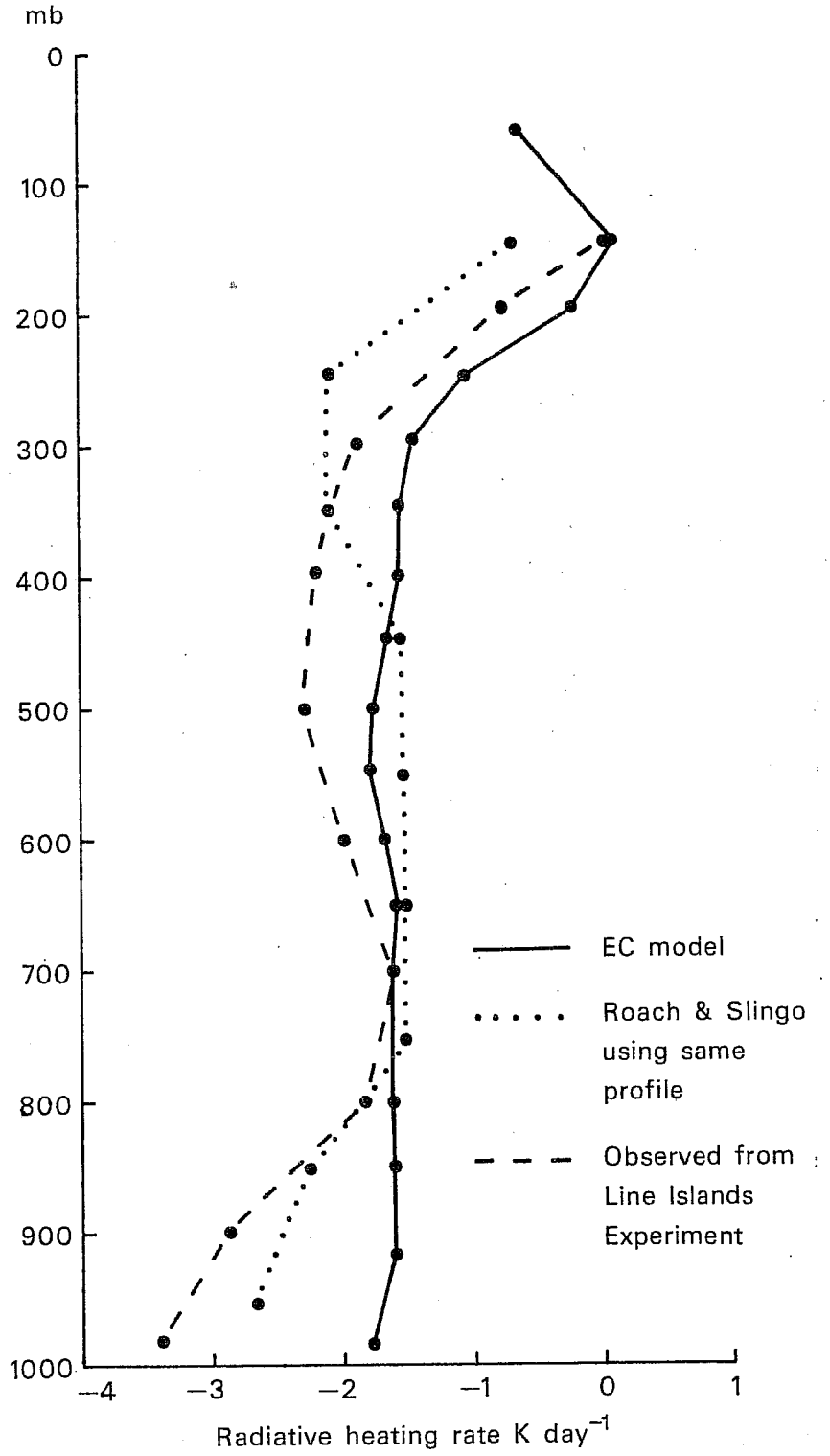

Fig. 4 Comparison of infra-red heating rates from EC scheme with other estimates.

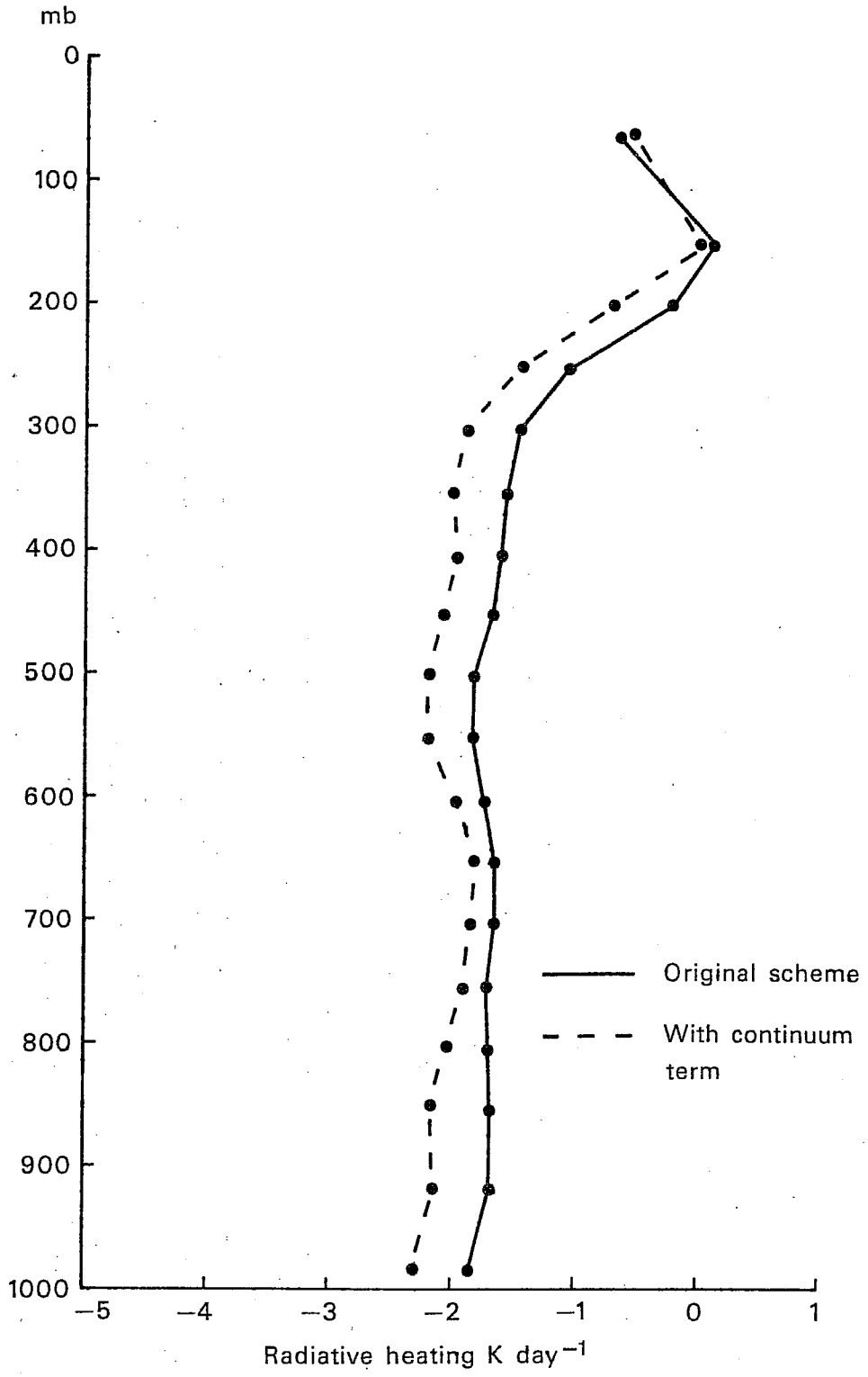

Fig. 5 Effect of including a simple continuum term on the infra-red heating rates.

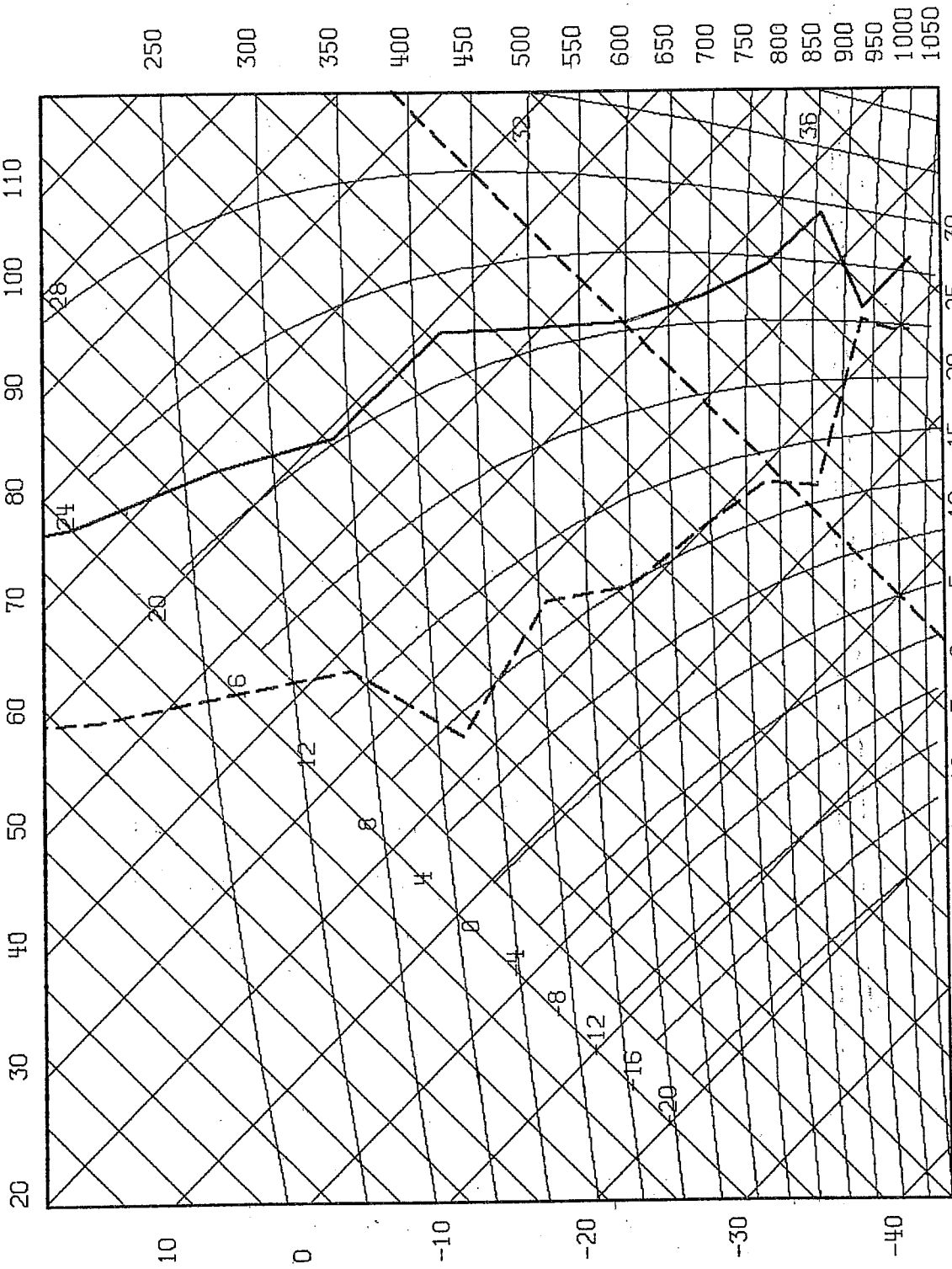

Fig. 6 ATEX profile.

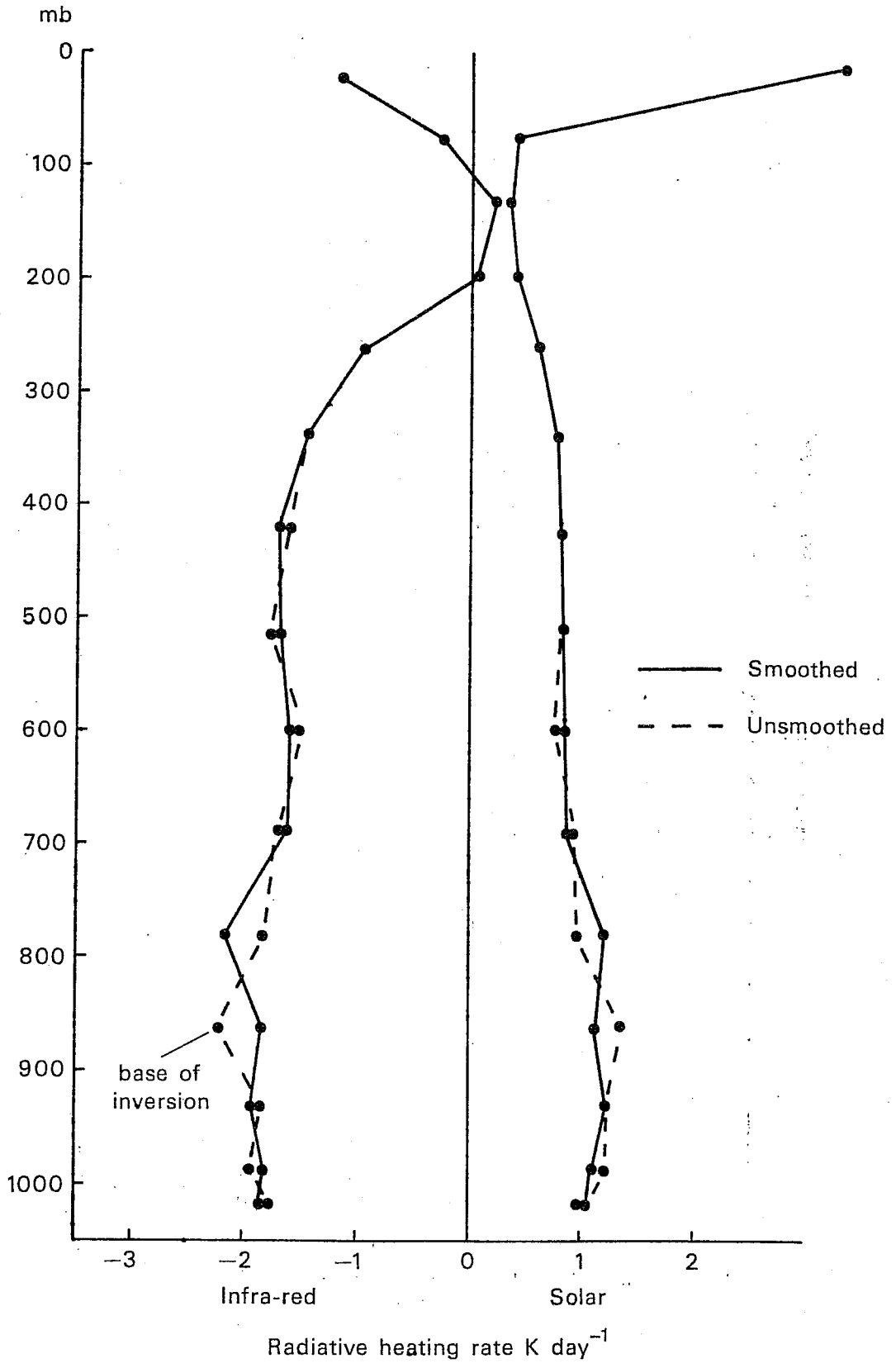

Fig. 7 Effect of vertical smoothing of humidity on the radiative heating associated with an atmospheric inversion.

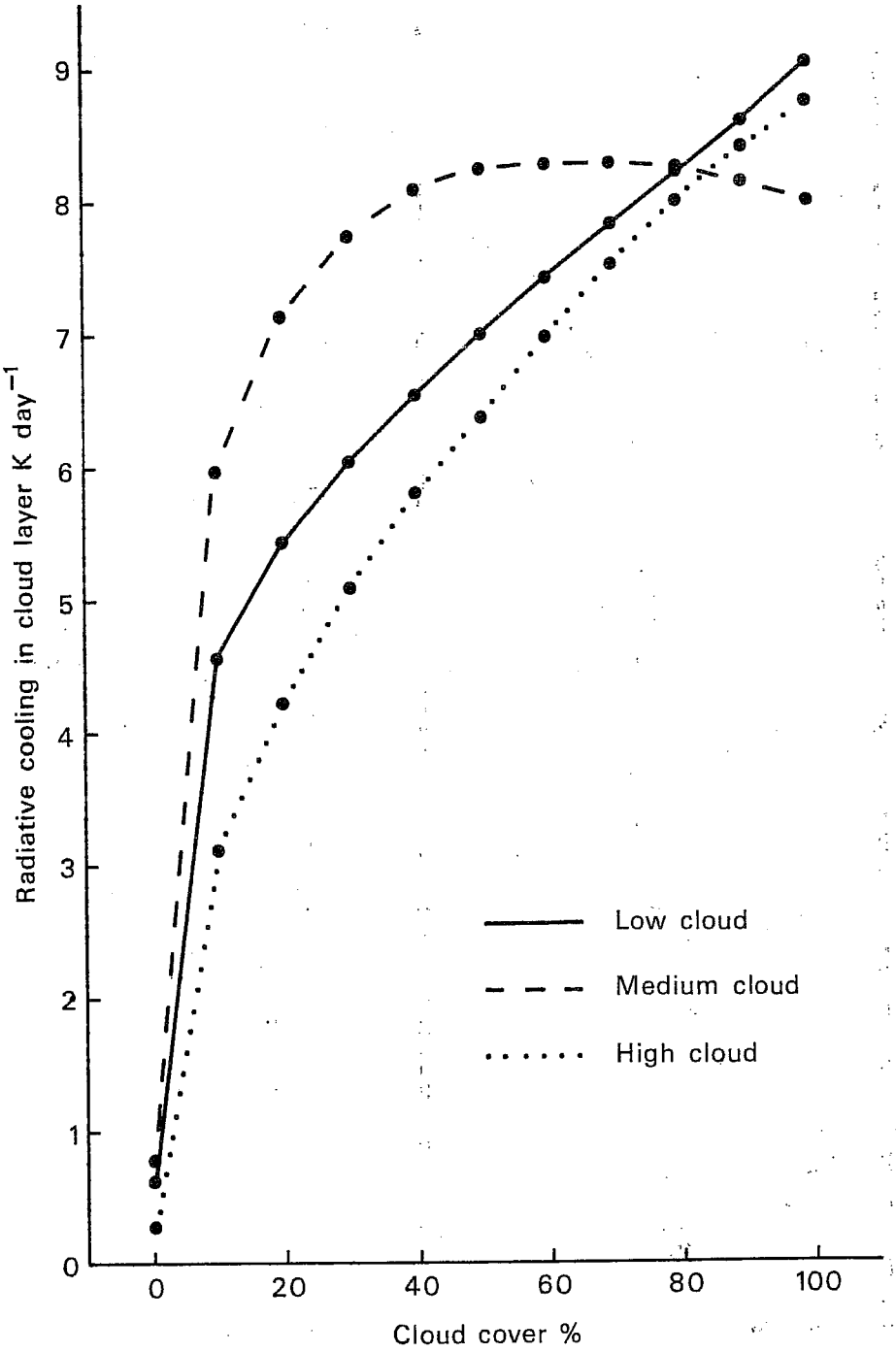

Fig. 8 Variation of radiative cooling in the cloud layer with cloud amount.

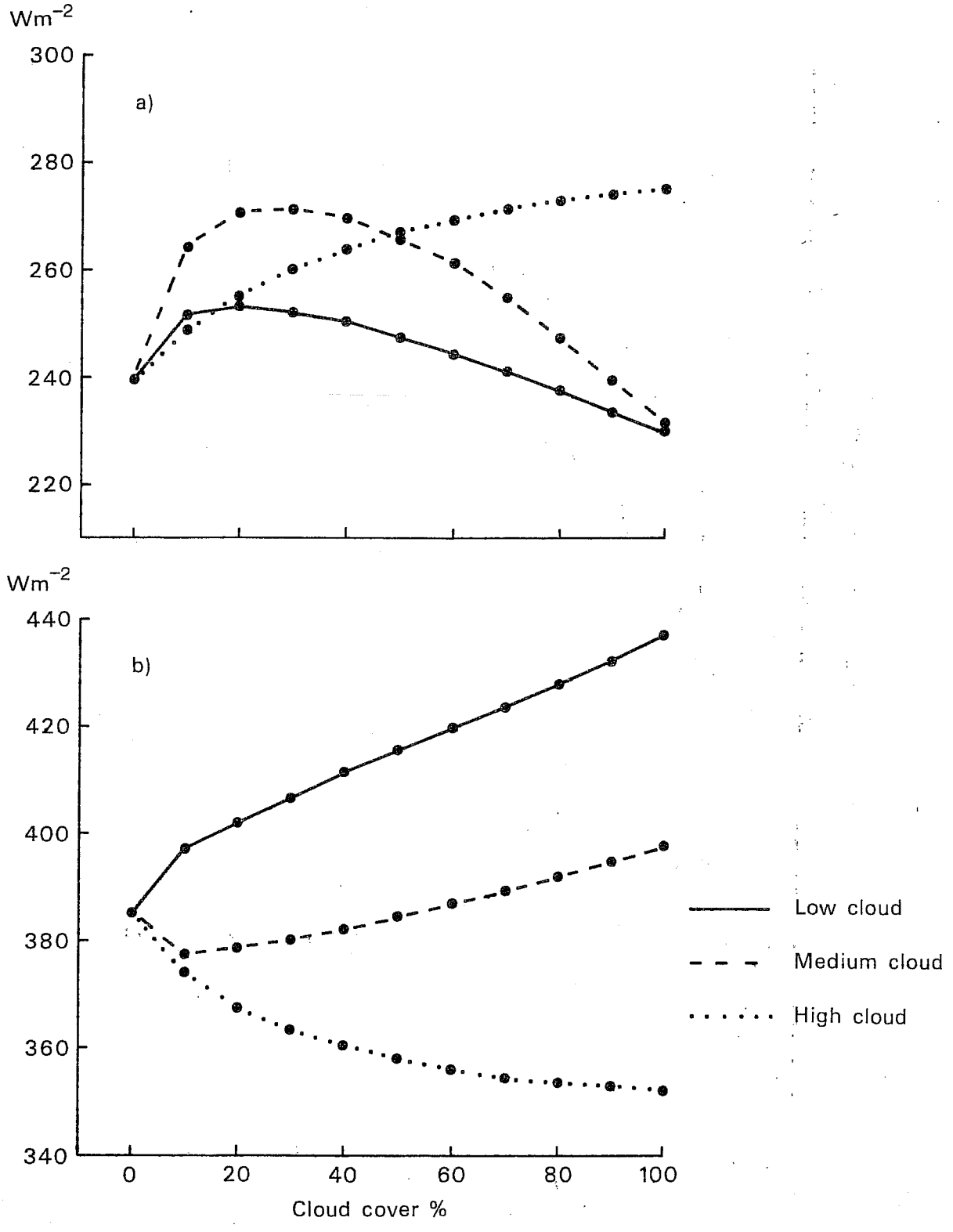

Fig. 9 Variation with cloud amount of a) outgoing flux at top of atmosphere and b) downward infra-red flux at surface.

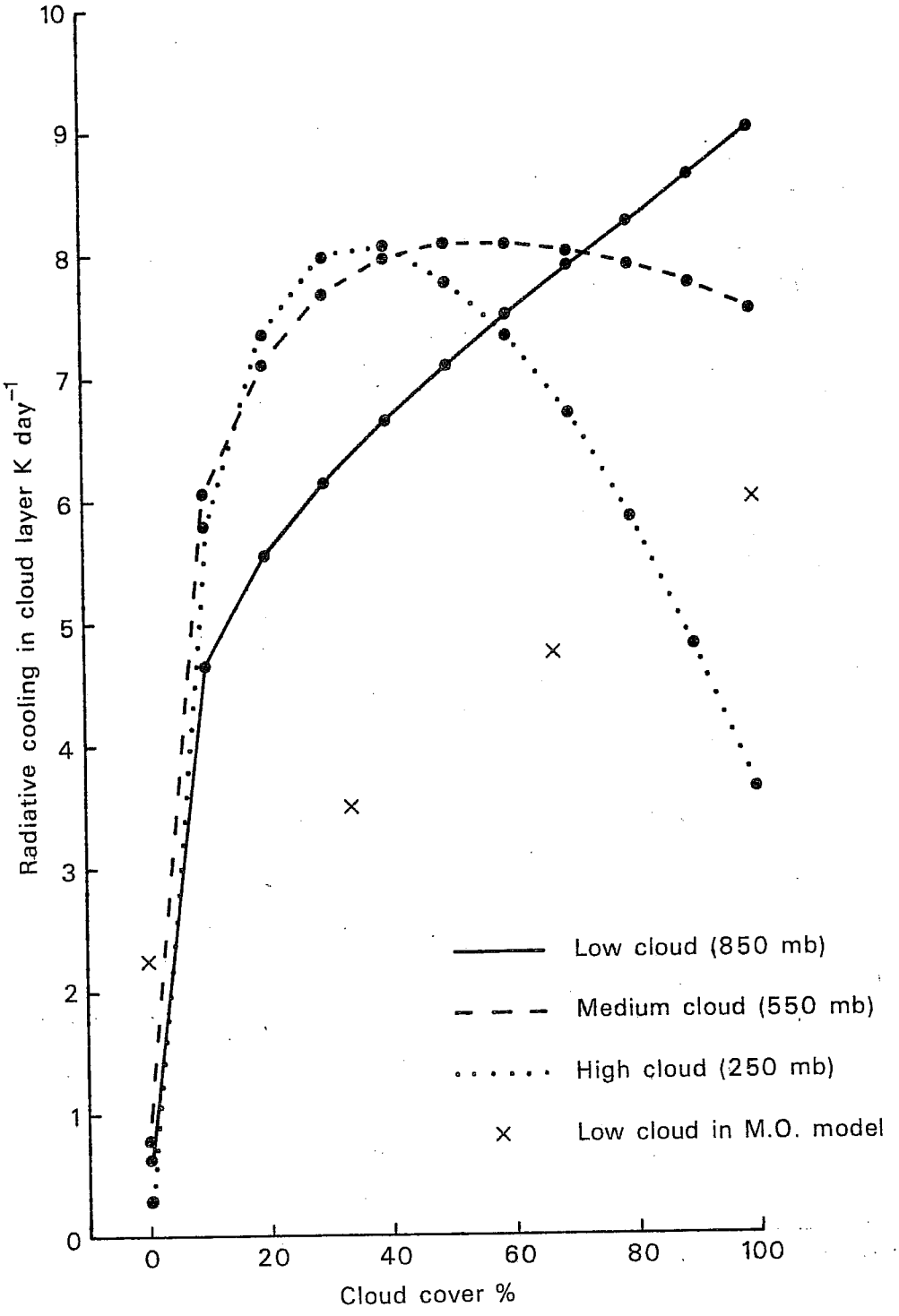

Fig. 10 Variation of net radiative cooling in cloud layer with cloud cover for revised liquid water contents.

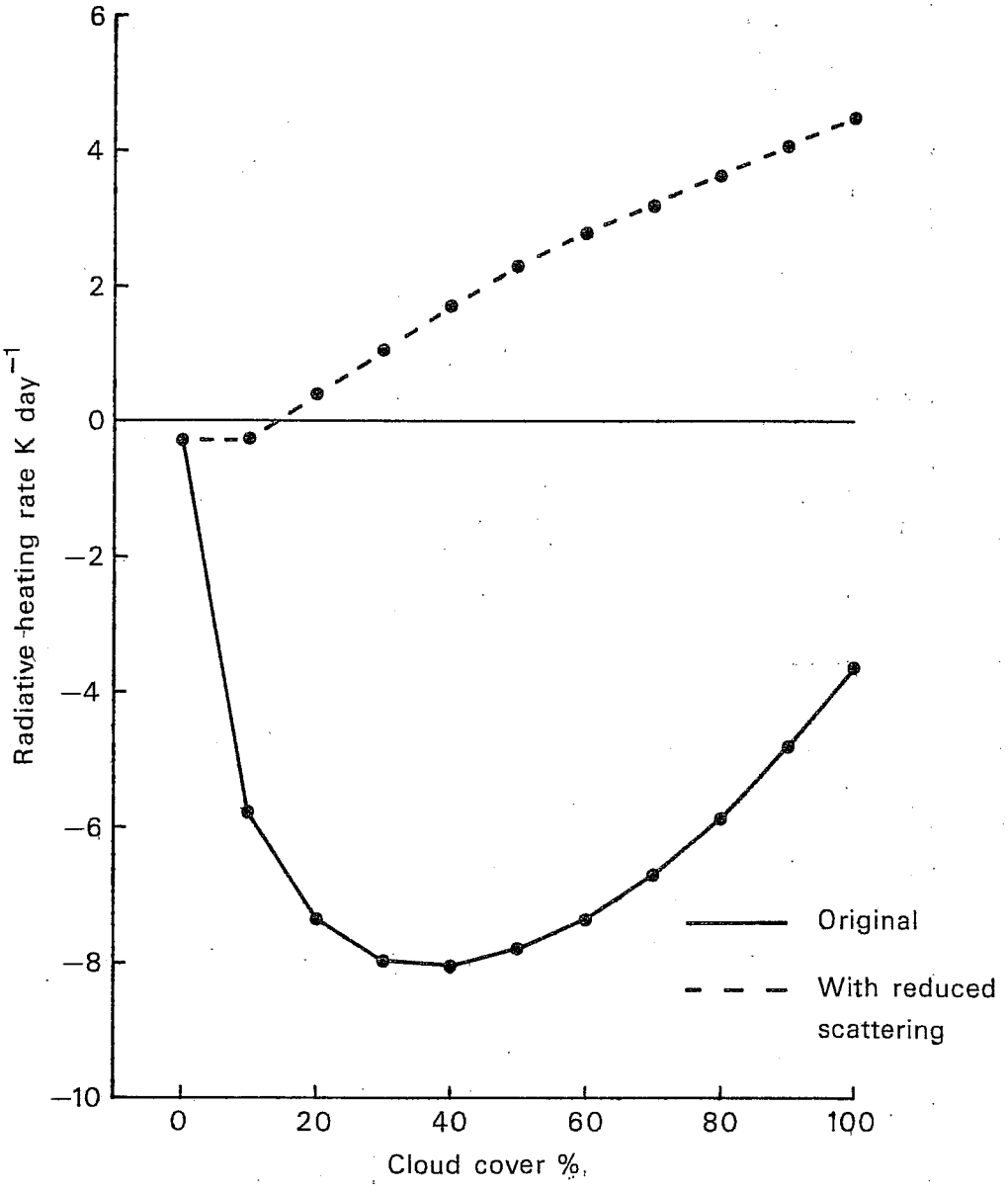

Fig. 11 Effect of reducing the single scattering albedo for high cloud on the radiative heating within the cloud.

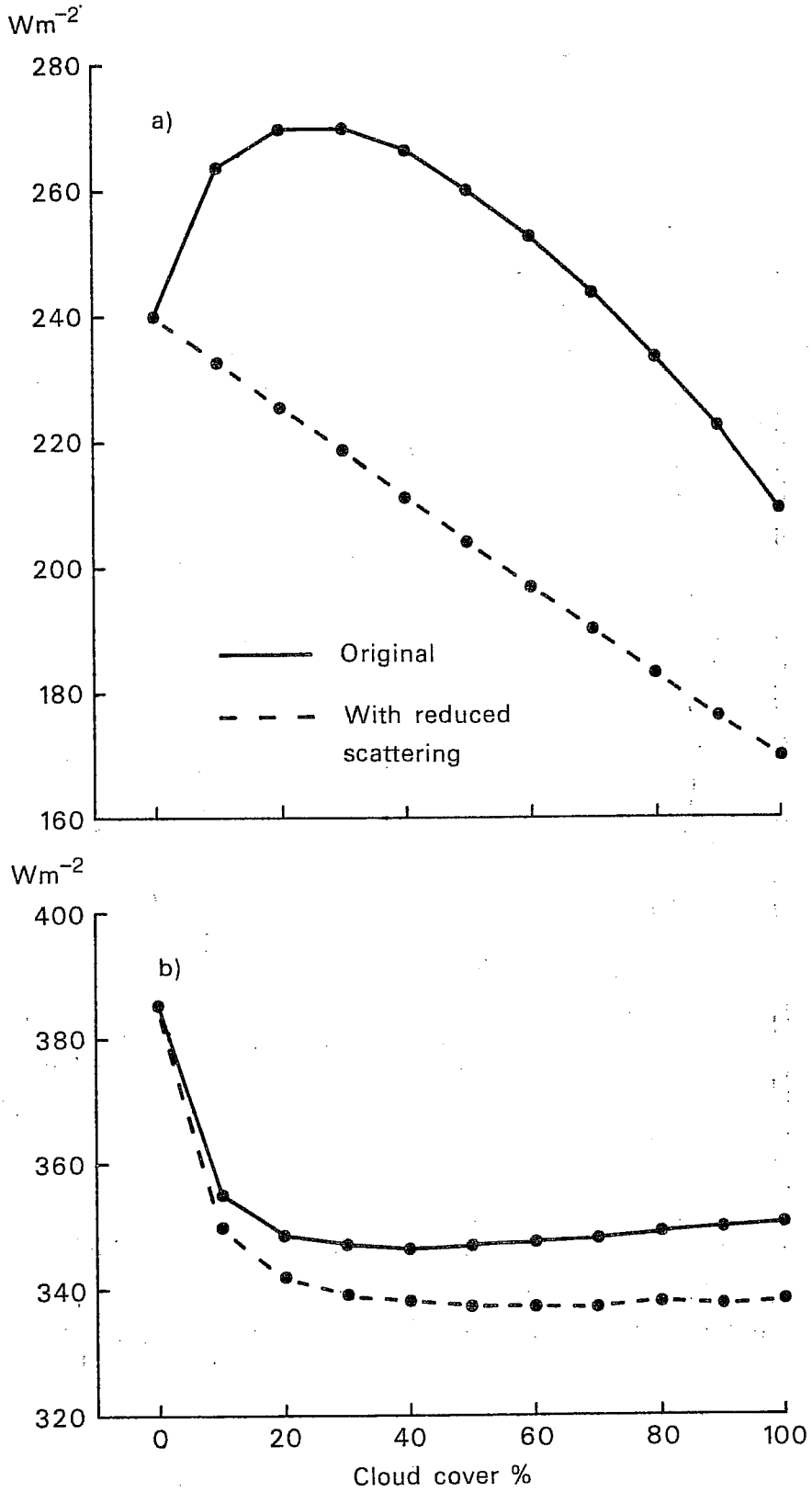

Fig. 12 Effect of reduced single scattering albedo for high cloud on a) outgoing long wave flux at top of atmosphere and b) downward long wave flux at surface.

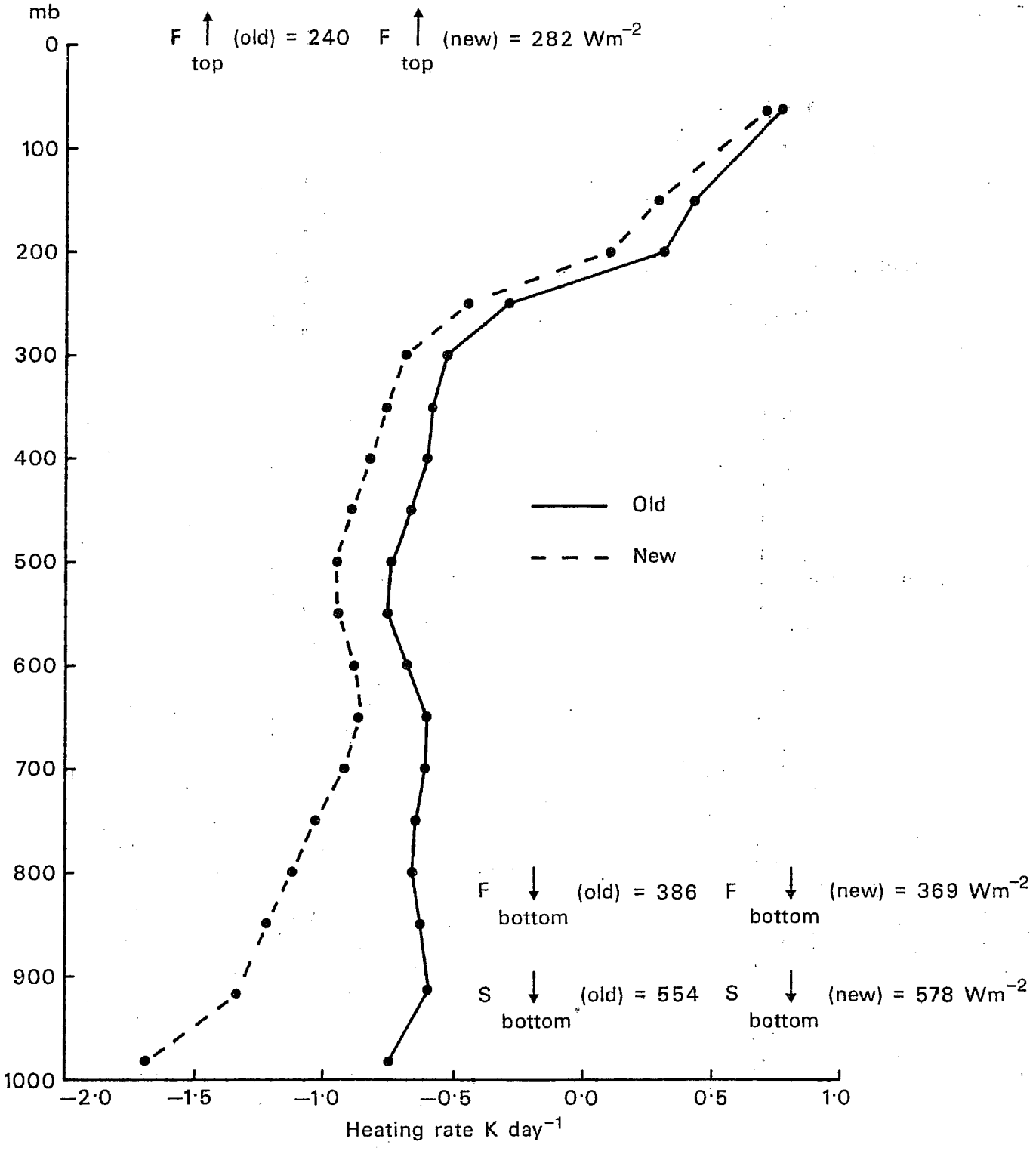

Fig. 13 Comparison of revised scheme with original scheme.

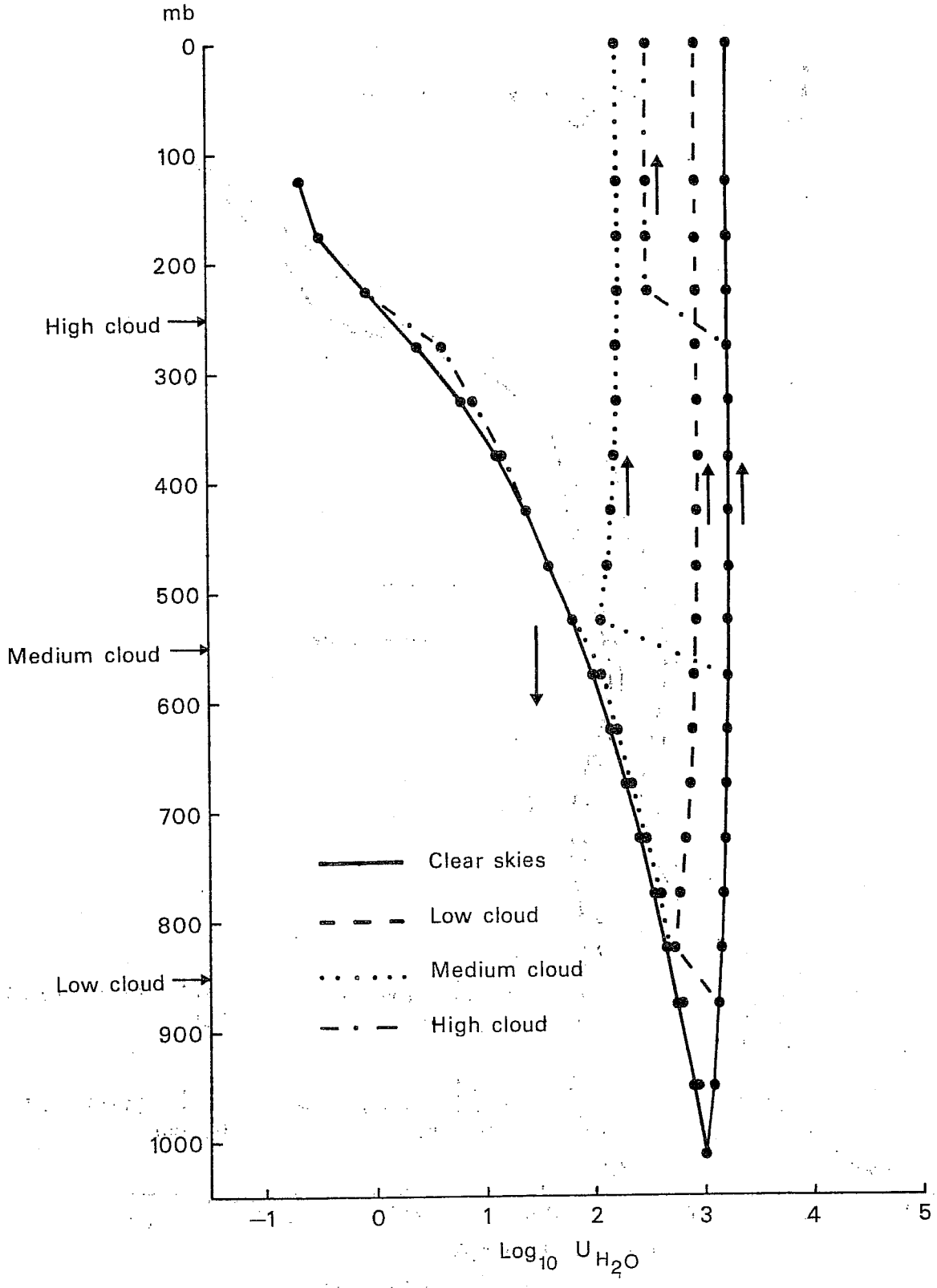

Fig. 14 Path lengths for the downward and upward infra-red radiation streams for clear and cloudy atmospheres.